Human amnion-derived mesenchymal stem cells promote osteogenic differentiation of lipopolysaccharide-induced human bone marrow mesenchymal stem cells via ANRIL/miR-125a/APC axis

Yuli Wang
Nanjing Medical University
Fengyi Lv
nanjjing medical university
Lintong Huang
nanjing medical university
Hengwei Zhang
university of rochester
Bing Li
nanjing medical university
Weina Zhou
nanjing medical university
Xuan Li
nanjing medical university
Yifei Du (duyifeinjmu@163.com)
Nanjing Medical University
Yongchu Pan
nanjing medical university
Ruixia Wang
nanjing medical university

Research

Keywords: Human amnion-derived mesenchymal stem cells, Human bone marrow mesenchymal stem cells, Lipopolysaccharide, Osteogenic differentiation, Long non-coding RNA ANRIL, microRNA-125a, Adenomatous polyposis coli, β-catenin

Posted Date: July 17th, 2020

DOI: https://doi.org/10.21203/rs.3.rs-42808/v1

Version of Record: A version of this preprint was published on January 7th, 2021. See the published version at https://doi.org/10.1186/s13287-020-02105-8.

Abstract

Background: Periodontitis is a chronic inflammatory disease inducing the absorption of alveolar bone and leading to tooth loss. Human amnion-derived mesenchymal stem cells (HAMSCs) have been studied as a potential strategy for inflammatory processes. Here, we explored the role of long non-coding RNA (LncRNA) antisense non-coding RNA in the INK4 locus (ANRIL) in HAMSCs-droved osteogenesis in lipopolysaccharide (LPS)-induced human bone marrow mesenchymal stem cells (HBMSCs).

Methods: Cells were incubated with coculture system. Reactive oxygen species (ROS) level and superoxide dismutase (SOD) activity were used to detect oxidative stress level. Flow cytometry was performed to determine the cell proliferation. The Alkaline phosphatase (ALP) and Alizarin red assay, cell transfection and rat mandibular defect model were used to evaluate the osteogenic differentiation. Quantitative real-time reverse transcription polymerase chain reaction (RT-PCR), Western blot, dual-luciferase reporter assay and immunofluorescence Staining were used to evaluate the molecular mechanisms.

Results: Here, we discovered that HAMSCs promoted osteogenesis of LPS-induced HBMSCs, while ANRIL level in HBMSCs was decreased during coculturing. ANRIL had no significant influence on the proliferation of LPS-induced HBMSCs, while its overexpression inhibited the HAMSCs-droved osteogenesis *in vivo* and *in vitro*; whereas its knockdown reversed these effects. Mechanistically, we found that downregulating ANRIL led to overexpression of microRNA-125a (miR-125a), and further contributed to the competitively bounding of miR-125a and Adenomatous polyposis coli (APC), thus significantly activating the Wnt/β-catenin pathway.

Conclusions: Our study indicates that HAMSCs promote osteogenic differentiation of LPS-induced HBMSCs *via* ANRIL/miR-125a/APC axis, and offer a novel approach for periodontitis therapy.

Introduction

Periodontitis is a group of plaque-induced chronic inflammatory process characterized by alveolar bone deficiency and tooth loss. So far, strategies for healing periodontitis are challenging, which may have remarkable individual differences and increase patients' burden. Lipopolysaccharide (LPS), the major virulence factor of the outer membranes of Gram-negative bacteria, is related with the immune responses of periodontitis(1, 2). Human bone marrow mesenchymal stem cells (HBMSCs) have commonly used in alveolar bone regeneration due to their self-renewal capacity and availability(3). However, pathological status induced by LPS is detrimental to HBMSCs retention and survival. Human amnion-derived mesenchymal stem cells (HAMSCs), harvested in a noninvasive way, have superior immunomodulatory properties and fewer ethical concerns(4). Our previous report found that HAMSCs modulated the osteogenic differentiation and alleviated oxidative stress in LPS-induced HBMSCs(5). Despite the research on driving HBMSCs osteogenesis against LPS by HAMSCs, the curative effect and regulatory mechanism still need to be fully investigated.

Long non-coding RNAs (lncRNAs) is a critical subgroup of non-coding RNAs (ncRNAs) more than 200 nucleotides in length(6), involve in a broad spectrum of biological control and pathology(7, 8). Antisense non-coding RNA in the INK4 locus (ANRIL) is a lncRNA that firstly found in melanoma and neural system tumor(9). Recent studies have indicated the relationship between ANRIL and periodontitis(10, 11).Higher level of ANRIL was found in porphyromonas gingivalis-induced periodontal tissue(12). Here, we investigated whether HAMSCs promoted osteogenesis of LPS-induced HBMSCs *via* ANRIL.

MicroRNAs (miRNAs) are a class of small non-coding RNAs that activate protein-encoding genes expression by binding to the (3' UTR) of the target mRNAs(13). Recent studies have demonstrated that ANRIL took part in the malignant transformation and progression of various diseases by acting as a sponge of MicroRNA-125a (miR-125a)(14, 15).However, whether ANRIL/miR-125a axis plays a role in the HAMSCs-droved osteogenesis remains undetermined. In this study, we investigated the effect of ANRIL and its underlying mechanism. We found that HAMSCs promoted osteogenic differentiation in LPS-induced HBMSCs while ANRIL decreased. Moreover, downregulating ANRIL induced miR-125a overexpression, further inhibiting Adenomatous polyposis coli (APC) and activating Wnt/β-catenin signaling. These new references for the lncRNA-miRNA-mRNA functional network could be a powerful strategy for the therapy of periodontitis.

Materials And Methods

Cell culture and co-culture system

All experiments were approved by the Ethics and Research Committee of Nanjing Medical University (Permit Number: 2018 – 190). Informed consent was obtained from all the participants. HAMSCs were obtained from discarded amniotic membrane and HBMSCs were collected from patients undergoing Sagittal Split Ramus Osteotomy (SSRO). Cells were isolated and maintained as reported(16, 17). 3–5 passages cells were used in this study. HAMSCs/HBMSCs transwell coculture system was established according to our previous research(5). After starvation in serum-free medium or LPS (1 μg/mL) for 24 h, HBMSCs were washed with PBS for subsequent experiments.

Quantitative Real-time Reverse Transcription Polymerase Chain Reaction (RT-PCR)

RNA isolation and cDNA transcribing were performed by TRIzol reagent (Invitrogen, New York, NY, USA) and Reverse Transcription Kit (Applied Biosystems, Foster City, CA). RT-PCR was conducted as reported(18). Primer sequences used are listed in Table 1. Human glyceraldehyde-3-phosphate dehydrogenase (GAPDH) was used as a reference for estimation of lncRNA and mRNAs, whereas human U6 was used to normalize miRNA. Fold changes in gene expression were determined by the $2^{-\Delta\Delta Ct}$ method.

Table 1

Genes	Sense primer(5′-3′)	Anti- sense primer(5′-3′)
ALP	AGAACCCAAAGGCTTCTTC	CTTGGCTTTTCCTTCATGGT
RUNX2	TCTTAGAACAAATTCTGCCCTTT	TGCTTTGGTCTTGAAATCACA
OCN	AGCAAAGGTGCAGCCTTTGT	GCGCCTGGGTCTCTTCACT
OSX	CCTCCTCAGCTCACCTTCTC	GTTGGGAGCCCAAATAGAAA
ANRIL	CCCTAGCTACATCCGTCACCTGA	CCACAGCTACATATGCGTTTACA
APC	AAAGTGAGCAGCTACCACG	CCTGGAGTGATCTGTTAGTCG
β-Catenin	AGCTGACAACTTTCACACC	AATGGGGATGTTGATCTTC

Primers used for quantitative real-time reverse transcription polymerase chain reaction.

Reactive oxygen species (ROS) level and superoxide dismutase (SOD) activity

Flow cytometry was used to determine LPS-induced ROS by measuring intensity of 2′,7′-dichlorofluorescin (DCF) fluorescence as reported(5). The SOD activity was detected using xanthine oxidase assay kit (Jiancheng Corp, Nanjing, China) according to the manufacturer's instructions(19).

Cell Transfection

Recombinant lentiviruses containing full-length ANRIL, scramble control (NC), targeting ANRIL and scramble control(shNC) were obtained from GenePharma Company (Shanghai, China). Those lentiviruses were named Lenti- ANRIL, Lenti-NC, Lenti-sh ANRIL and Lenti-shNC, respectively. HBMSCs transferred with MiRNA plasmids (Ribobio, Guangzhou, China) were prepared by transfection reagent riboFECTTM CP (Ribobio, Guangzhou, China). The mutated binding sites of miR-125a in luciferase reporter vectors containing APC were constructed by site-directed mutagenesis.

Cell Proliferation Assay

HBMSCs were collected at 1,3 and 5d. Flow cytometry (BD Biosciences, Franklin Lakes, NJ, USA) was performed to determine the cell viability as reported(20). G0, G1, S, and G2 M phases were determined using MODFIT LT 3.2 (Verity Software House, Topsham, ME, USA).

Alkaline Phosphatase (ALP) And Alizarin Red Assay

After 7 days osteogenic inducing, ALP staining and activity was detected using NBT/BCIP staining kit (CoWin Biotech, Beijing, China) and ALP assay kit (Jiancheng Corp, Nanjing, China) as reported(21, 22). Mineralized matrix formation was determined after 14 days osteogenic inducing as reported(23).

Western Blot

Western blot analysis was performed as reported(24). The primary antibodies were: anti-ALP (ab83259) (1:1000),anti-osteocalcin (OCN) (ab133612) (1:1000), anti- Osterix(OSX) (ab209484) (1:1000)(All from Abcam, Cambridge, MA, USA).RUNX2 (D1L7F) Rabbit mAb #12556(1:1000), APC Antibody #2504(1:1000), β-Catenin (D10A8) XP® Rabbit mAb #8480(1:1000),β-actin (8H10D10) Mouse mAb #3700(1:1000)(All from Cell Signaling Technology ,Danvers, MA,USA).β-actin served as an internal control.

In vivo bone formation assay

Approximately 10×10^4 cells (5×10^4 HAMSCs and 5×10^4 $HBMSCs^{NC}$/$HBMSCs^{ANRIL}$/ $HBMSCs^{shNC}$/$HBMSCs^{shANRIL}$ pretreated with LPS) were attached to each HA/TCP biomaterial (Φ5 × H2mm, Sichuan University, Chengdu, Sichuan, China). After 12 hours, the complexes were subcutaneously implanted into the rat mandibular defect area designed as reported (4 female nude rats per group, with an average weight of 280 g)(23). All animal experiments were done in compliance with the regulations and guidelines of Nanjing Medical University institutional animal care.

Micro Computed Tomography (micro-CT) Analysis

Mandibles were harvested for micro-CT analysis after 8 weeks implantation as reported(25). Bone volume ratio (BV/ TV, %) was calculated.

Histological Observation

Mandible samples were harvested and analyzed by hematoxylin and eosin (H&E), Masson trichrome and immunohistochemistry. Primary antibodies against RUNX2 (1:300 dilution) were used for immunohistochemistry as reported(23). Positive areas were observed under the microscope.

Dual-luciferase Reporter Assay

Luciferase assays were performed by Lipofectamine 2000 and Dual Luciferase Reporter Assay System as reported(26).

Immunofluorescence Staining

Primary antibody [β-Catenin (D10A8) XP® Rabbit mAb #8480(1:100), Cell Signaling Technology, Danvers, MA, USA] and DAPI were used to perform immunofluorescence staining as reported(23). Images were captured under the inverted fluorescence microscope (Olympus, Japan).

Statistical analysis

The data are expressed as the mean and standard deviation (SD) of at least three independent samples. $p < 0.05$ was considered statistically significant using Student's t-test or ANOVA analysis.

Results

LncRNA-ANRIL expression in LPS-induced HBMSCs decreases with the HAMSCs coculturing

To verify the previous findings that HAMSCs reduced oxidative stress and promoted osteogenic differentiation in LPS-induced HBMSCs, we established transwell coculture model and detected related markers. HAMSCs increased the expression of osteogenic markers, including ALP, RUNX2 and OCN (Fig. 1A). In addition, HAMSCs also decreased the oxidative stress level induced by LPS in HBMSCs, which were confirmed by ROS and SOD measuring (Fig. 1B, C). Meanwhile, RT-PCR showed that levels of ANRIL in LPS-induced HBMSCs significantly decreased in a time-dependent manner along with the HAMSCs coculturing (Fig. 1D).

LncRNA-ANRIL Has No Effects On LPS-induced HBMSCs Proliferation

Then, stably expressing cells ($HBMSCs^{NC}$, $HBMSCs^{ANRIL}$, $HBMSCs^{shNC}$ and $HBMSCs^{shANRIL}$) were sorted and cocultured with HAMSCs after LPS pretreatment. Cells were assigned into: HBMSCs; LPS: LPS + HBMSCs; HAMSCs: HAMSCs + LPS + HBMSCs; NC: HAMSCs + LPS + $HBMSCs^{NC}$; ANRIL: HAMSCs + LPS + $HBMSCs^{ANRIL}$; shNC: HAMSCs + LPS + $HBMSCs^{shNC}$; shANRIL: HAMSCs + LPS + $HBMSCs^{shANRIL}$. Proliferation assay determined by flow cytometry suggested HAMSCs promoted growth of LPS-induced HBMSCs, while no significant difference in S-phase checkpoints was detected among HAMSCs, NC, ANRIL, shNC and shANRIL group (Fig. 1E).

HAMSCs promote osteogenesis of LPS-induced HBMSCs via downregulation LncRNA-ANRIL

Osteogenic differentiation in HBMSCs play a key role in reversing alveolar bone deficiency. Thus, we investigated whether ANRIL could take part in HAMSCs-droved osteogenesis. HAMSCs enhanced ALP staining and activity compared with those in LPS groups, whereas ANRIL overexpression in HBMSCs inhibited the effect and ANRIL knockdown promoted it (Fig. 2A).Besides, Alizarin red staining and quantification showed decreased matrix mineralization in the ANRIL group compared with those in HAMSCs and NC groups, whereas ANRIL knockdown showed the opposite effects (Fig. 2B). RT-PCR and Western blot assay showed that the mRNA and protein levels of ALP, RUNX2 (early-stage osteogenic markers) and OCN, OSX (late-stage marker) were decreased by ANRIL overexpression and increased by ANRIL knockdown (Fig. 2C, D).

Followed the *in vitro* study, we examined the effect of ANRIL *in vivo* by mandibular defect model (Fig. 3A). Percentage of mineralized volume fraction was measured. ANRIL decreased bone volume/total volume (BV/TV) compared with the NC group, while increased BV/TV was detected in the shANRIL group compared with shNC (Fig. 3B). H&E and Masson staining showed less organized bone matrix and more fibrous tissue in the ANRIL group, while shANRIL group exhibited better bone formation. Immunohistochemistry also confirmed RUNX2 expression was downregulated in the ANRIL group compared to NC group and upregulated in the shANRIL group compared to shNC group (Fig. 3C).

MiR-125a is a downstream negatively correlated with LncRNA-ANRIL

We next investigated the possible interaction between ANRIL and miR-125a. Putative miR-125a binding sequence of ANRIL was predicated by Target Scan software (Fig. 4A). miR-125a expression was downregulated by ANRIL overexpression and upregulated by ANRIL knockdown (Fig. 4B). After that, miR-125a mimics and inhibitor were transfected into HBMSCs and the transfection efficacy was detected by RT-PCR (Fig. 4C).Cells were assigned into NC: HAMSCs + LPS + HBMSCs$^{miR-125a\ NC}$; mimics: HAMSCs + LPS + HBMSCs$^{miR-125a\ mimics}$; iNC: HAMSCs + LPS + HBMSCs$^{miR-125a\ iNC}$; inhibitor: HAMSCs + LPS + HBMSCs$^{miR-125a\ inhibitor}$. miR-125a mimics enhanced ALP staining and activity compared with those in NC groups, whereas miR-125a inhibitor in HBMSCs inhibited the effect (Fig. 4D). Besides, Alizarin red staining and quantification showed increased matrix mineralization in the miR-125a mimics group compared with those in NC groups, whereas miR-125a inhibitor showed the opposite effects (Fig. 4E). RT-PCR and Western blot assay showed that the mRNA and protein levels of ALP, RUNX2 (early-stage osteogenic markers) and OCN, OSX (late-stage marker) were increased by miR-125a inhibitor and decreased by miR-125a inhibitor (Fig. 4F, G).

MiR-125a alleviates HAMSCs-droved osteogenesis in HBMSCs by targeting APC and activating Wnt/β-catenin pathway

APC was searched as the candidate target gene of miR-125a by Target Scan software (Fig. 5A). Western blot assay and RT-PCR showed that the mRNA and protein levels of APC were significantly decreased by miR-125a mimics and increased by miR-125a inhibitor (Fig. 5B, C). We further studied the mechanisms on miR-125a-APC interaction and performed a dual luciferase reporter assay. The results suggested that miR-125a mimics reduced luciferase activity of APC wild-type reporter, while this suppressive effect was rescued by mutation of the putative miR-125a target sites (Fig. 5D).

As APC is a negative regulator in Wnt/β-catenin pathway(27), APC overexpression was established in HBMSCs and cells were assigned into NC: HAMSCs + LPS + HBMSCs$^{APC\ NC}$; APC: HAMSCs + LPS + HBMSCs^{APC}. Western blot assay determined that APC overexpression increased the protein level of APC and decreased the protein level of β-catenin (Fig. 5E).However, the mRNA level of β-catenin was stably, which suggested APC overexpression only induced β-catenin protein degradation without influencing mRNA (Fig. 5F).Immunofluorescence staining further showed a significantly decrease in nuclear β-catenin accumulation when APC overexpressed (Fig. 5G).Moreover, Western blot assay and RT-PCR showed that the protein and mRNA levels of ALP, RUNX2 (early-stage osteogenic markers) and OCN, OSX (late-stage marker) were decreased by APC overexpression (Fig. 5H, I).

MiR-125a inhibitor suppresses the APC downregulating and osteogenesis caused by shANRIL

The rescue assays were carried out to help us fully understand the role of miR-125a and APC involved in ANRIL-mediated osteogenesis. As shown in Fig. 6A, B, shANRIL and miR-125a inhibitor co-transfection rectified APC suppression compared to the shANRIL group. shANRIL-mediated osteogenic markers expression could also be partly inhibited in co-transfected cells (Fig. 6B, C). shANRIL enhanced ALP staining and activity compared with those in shNC groups, whereas co-transfection partly inhibited the effect (Fig. 6D). Besides, Alizarin red staining and quantification showed decreased matrix mineralization in the co-transfection group compared with those in shANRIL groups (Fig. 6E). Taken together, HAMSCs downregulates lncRNA-ANRIL in LPS-induced HBMSCs, upregulates the miR-125a level, targets APC transcription, and activates the Wnt/β-catenin pathway to induce new bone formation.

Discussion

The present study demonstrated that lncRNA-ANRIL derived from LPS-pretreated HBMSCs was responsible for HAMSCs-induced osteogenesis. Briefly, HAMSCs promoted osteogenesis and reduced oxidative stress in LPS-pretreated HBMSCs, and lncRNA-ANRIL in HBMSCs was significantly decreased with the HAMSCs co-culturing. Then, application of HAMSCs + LPS + HBMSCs^{shANRIL} into scaffold material induced bone formation in mandibular defect. Furthermore, miR-125a, acting as a sponge of ANRIL, not only regulated HBMSCs function in osteogenesis by targeting APC, but also positively regulated osteogenic differentiation by the Wnt/β-catenin pathway, which suggests the axis may be a potentially biological target for treating inflammatory-related bone deficiency (Fig. 7). Periodontitis is the

most prevalent disease of the alveolar bone, which eventually leads to periodontal tissue and tooth loss. Yet, the present strategies, such as autologous bone and biomaterials transplantation, suffer from limited sources, uncertain outcomes and high cost(28, 29).Tissue regeneration based on stem cells is a promising therapy approach. It has been reported that HAMSCs, isolated from amniotic membrane, is associated with superior immunomodulatory properties and less ethical controversy(4, 30) .Previous study also indicate that decreased inflammation factors and increased growth factors are the potentially causes of HAMSCs implication in tissue remodeling(30). At the beginning of this study, we observed that the osteogenic differentiation and oxidative stress of LPS-induced HBMSCs were significantly alleviated with HAMSCs coculturing, which were consist with our previous investigation(31). Importantly, these phenotypic changes in LPS-induced HBMSCs were accompanied by progressively reduced lncRNA-ANRIL expression.

Next, we concern lncRNA-ANRIL as a significant aspect of our study. ANRIL, formerly regarded as risk locus associated with coronary heart disease and germline deletion by genome wide association studies(9, 32),is located a 42-kb stretch within the chromosomal region 9p21.3.As periodontitis and coronary heart disease share similar pathogenic bacterial strains, environmental and behavioural risk factors(33, 34),recent research give suggestive evidence for a positive correlation between ANRIL and periodontitis across different populations(11). Furthermore, enhanced ANRIL transcription in bacterial-infected periodontal tissue is upregulated by multiple signaling pathways response to inflammation(35).According to the anti-inflammatory properties of HAMSCs and decreased ANRIL expression in LPS-induced HBMSCs, we tested whether HAMSCs performed its' function through ANRIL. In our study, HBMSCs^{ANRIL} gave rise to reversed osteogenssis, while HBMSCs^{shANRIL} showed the opposite effects. Thus, these data demonstrate that HAMSCs contributes to LPS-induced HBMSCs osteoblastogenesis by reducing ANRIL expression.

In the past few years, lncRNAs have been indicated as miRNA sponges to negatively regulate miRNA expression(36). MiRNAs are involved in multiple cellular processes by influencing gene expression(37). Thus, we hypothesized that the effects of ANRIL might be associated with miRNA expression. MiR-125a can take part in cell proliferation, differentiation and senescence by influencing mRNA stability and translation(38). It has been reported that inhibition of ANRIL induced cell apoptosis, which is possibly correlated with increased miR-125a expression(15).Additionally, association of miR-125a and periodontitis has been investigated in a previous study(39). We demonstrated that miR-125a in LPS-induced HBMSCs was direct bound by ANRIL and negatively regulated. MiR-125a mimics not only led to elevated ANRIL expression but also increased osteogenesis. Furthermore, miR-125a inhibitor not only upregulated ANRIL expression but also reversed osteogenic differentiation caused by HAMSCs. Collectively, all these data indicate that ANRIL acts as a miR-125a sponge in the underlying mechanism.

Wnt/β-catenin pathway is a classic signal exerts multiple roles in cellular behaviors(40, 41). APC, which act as a negative regulator in Wnt/β-catenin, notably binds to β-catenin and inhibits its' unclear transferring(42). Targeting APC may emerge as external stimuli, promote nuclear localization of β-catenin, and activate the pathway. In this study, we confirmed that miR-125a bound to the 3'UTR of APC,

and their expression were negative correlated. Then, we explored the roles of APC and β-catenin involved in the mechanism. Our results suggested that APC overexpression intuitively decreased nuclear localization of β-catenin and contributed to osteoblast repression in HBMSCs. Moreover, the rescue assays showed that shANRIL and miR-125a inhibitor co-transfection rectified APC suppression and inhibited osteogenic differentiation. Thus, we believe that the interaction between APC and β-catenin serves as a downstream of miR-125a in ANRIL-induced osteogenesis.

Conclusion

In conclusion, our findings support the hypothesis that HAMSCs promote osteogenic differentiation of LPS-induced HBMSCs *via* lncRNA-ANRIL /miR-125a/APC/β-catenin axis. Based on these results, we might propose a viable therapeutic target and paramount approach for the therapy of inflammatory bone-destructive processes.

Abbreviations

LPS: lipopolysaccharide; HBMSCs: human bone marrow mesenchymal stem cells; HAMSCs: human amnion-derived mesenchymal stem cells; LncRNAs: Long non-coding RNAs; NcRNAs: non-coding RNAs; ANRIL: antisense non-coding RNA in the INK4 locus; MiRNAs: microRNAs; MiR-125a: microRNA-125a; APC: adenomatous polyposis coli; SSRO: sagittal Split Ramus Osteotomy; GAPDH: glyceraldehyde-3-phosphate dehydrogenase; ROS: reactive oxygen species; SOD: superoxide dismutase; DCF: 2',7'-dichlorofluorescin; RT-PCR: quantitative real-time reverse transcription polymerase chain reaction; ALP: alkaline phosphatase; OCN: osteocalcin; OSX: osterix; Micro-CT: micro computed tomography; H&E: hematoxylin and eosin; BV/TV: bone volume/total volume.

Declarations

Availability of data and materials

All other relevant datasets have been uploaded as part of additional files.

Ethics approval and consent to participate

All human stem cells involved in the present research followed the International Society for Stem Cell Research "Guidelines for the Conduct of Human Embryonic Stem Cell Research." The study was approved by the Ethics and Research Committee of Nanjing Medical University approved the study protocols (Permit Number: 2018 – 190). Informed consent was obtained from all the participants.

Consent for publication

Not applicable.

Competing interests

The authors declare no conflicts of interest.

Funding

This work was supported by grants from the Priority Academic Program Development of Jiangsu Higher Education Institutions (PAPD, No. 2018 – 87), the Jiangsu Provincial Commission of Health and Family Planning, Nanjing, China (No. BJ18035), the National Natural Science Foundation of China (No. 81800936), the Natural Science Foundation of Jiangsu Province (No. BK20180668, BK20190648), the Southeast University-Nanjing Medical University Cooperative Research Project (No. 2242018K3DN17), China Postdoctoral Science Foundation Funded Project (No. 2018M64050 and 2019T120445), Jiangsu Postdoctoral Science Foundation Funded Project (No. 2018K251C), the Jiangsu Province Undergraduate Innovation and Entrepreneurship Training Program (No. 201910312004Z), and the Open Research Fund of Jiangsu Key Laboratory of Oral Diseases (No. JSKLOD-KF-1903).

Authors’ contributions

Yuli Wang performed the experiments; Fengyi Lv and Lintong Huang supervised the study; Hengwei Zhang, Bing Li and Weina Zhou interpreted the data, and wrote the original draft; Xuan Li performed some experiments and data analysis; Yifei Du designed the experiments; Yongchu Pan and Ruixia Wang wrote the manuscript. All authors have read and approved the final version of the manuscript.

Acknowledgements

Not applicable.

References

1. Hajishengallis G. Immunomicrobial pathogenesis of periodontitis: keystones, pathobionts, and host response. Trends Immunol. 2014;35(1):3–11.
2. How KY, Song KP, Chan KG. Porphyromonas gingivalis: An Overview of Periodontopathic Pathogen below the Gum Line. Front Microbiol. 2016;7:53.
3. Macchiarini P, Jungebluth P, Go T, Asnaghi MA, Rees LE, Cogan TA, et al. Clinical transplantation of a tissue-engineered airway. Lancet. 2008;372(9655):2023–30.

4. Lobo SE, Leonel LC, Miranda CM, Coelho TM, Ferreira GA, Mess A, et al. The Placenta as an Organ and a Source of Stem Cells and Extracellular Matrix: A Review. Cells Tissues Organs. 2016;201(4):239–52.
5. Wang Y, Wu H, Shen M, Ding S, Miao J, Chen N. Role of human amnion-derived mesenchymal stem cells in promoting osteogenic differentiation by influencing p38 MAPK signaling in lipopolysaccharide -induced human bone marrow mesenchymal stem cells. Exp Cell Res. 2017;350(1):41–9.
6. Schmitz SU, Grote P, Herrmann BG. Mechanisms of long noncoding RNA function in development and disease. Cell Mol Life Sci. 2016;73(13):2491–509.
7. Fatica A, Bozzoni I. Long non-coding RNAs: new players in cell differentiation and development. Nat Rev Genet. 2014;15(1):7–21.
8. Geisler S, Coller J. RNA in unexpected places: long non-coding RNA functions in diverse cellular contexts. Nat Rev Mol Cell Biol. 2013;14(11):699–712.
9. Pasmant E, Laurendeau I, Heron D, Vidaud M, Vidaud D, Bieche I. Characterization of a germ-line deletion, including the entire INK4/ARF locus, in a melanoma-neural system tumor family: identification of ANRIL, an antisense noncoding RNA whose expression coclusters with ARF. Cancer Res. 2007;67(8):3963–9.
10. Bochenek G, Hasler R, El Mokhtari NE, Konig IR, Loos BG, Jepsen S, et al. The large non-coding RNA ANRIL, which is associated with atherosclerosis, periodontitis and several forms of cancer, regulates ADIPOR1, VAMP3 and C11ORF10. Hum Mol Genet. 2013;22(22):4516–27.
11. Schaefer AS, Bochenek G, Manke T, Nothnagel M, Graetz C, Thien A, et al. Validation of reported genetic risk factors for periodontitis in a large-scale replication study. J Clin Periodontol. 2013;40(6):563–72.
12. Schaefer AS, Richter GM, Dommisch H, Reinartz M, Nothnagel M, Noack B, et al. CDKN2BAS is associated with periodontitis in different European populations and is activated by bacterial infection. J Med Genet. 2011;48(1):38–47.
13. Lou G, Dong X, Xia C, Ye B, Yan Q, Wu S, et al. Direct targeting sperm-associated antigen 9 by miR-141 influences hepatocellular carcinoma cell growth and metastasis via JNK pathway. J Exp Clin Cancer Res. 2016;35:14.
14. Li R, Yin F, Guo YY, Zhao KC, Ruan Q, Qi YM. Knockdown of ANRIL aggravates H2O2-induced injury in PC-12 cells by targeting microRNA-125a. Biomed Pharmacother. 2017;92:952–61.
15. Hu X, Jiang H, Jiang X. Downregulation of lncRNA ANRIL inhibits proliferation, induces apoptosis, and enhances radiosensitivity in nasopharyngeal carcinoma cells through regulating miR-125a. Cancer Biol Ther. 2017;18(5):331–8.
16. Zhang D, Jiang M, Miao D. Transplanted human amniotic membrane-derived mesenchymal stem cells ameliorate carbon tetrachloride-induced liver cirrhosis in mouse. PLoS One. 2011;6(2):e16789.
17. Akintoye SO, Lam T, Shi S, Brahim J, Collins MT, Robey PG. Skeletal site-specific characterization of orofacial and iliac crest human bone marrow stromal cells in same individuals. Bone.

2006;38(6):758–68.

18. Dong X, Jin Z, Chen Y, Xu H, Ma C, Hong X, et al. Knockdown of long non-coding RNA ANRIL inhibits proliferation, migration, and invasion but promotes apoptosis of human glioma cells by upregulation of miR-34a. J Cell Biochem. 2018;119(3):2708–18.
19. Zhao Q, Shao L, Hu X, Wu G, Du J, Xia J, et al. Lipoxin a4 preconditioning and postconditioning protect myocardial ischemia/reperfusion injury in rats. Mediators Inflamm. 2013;2013:231351.
20. Wang J, Miao J, Meng X, Chen N, Wang Y. Expression of long noncoding RNAs in human bone marrow mesenchymal stem cells cocultured with human amnionderived mesenchymal stem cells. Mol Med Rep. 2017;16(5):6683–9.
21. Ge W, Shi L, Zhou Y, Liu Y, Ma GE, Jiang Y, et al. Inhibition of osteogenic differentiation of human adipose-derived stromal cells by retinoblastoma binding protein 2 repression of RUNX2-activated transcription. Stem Cells. 2011;29(7):1112–25.
22. Ge W, Liu Y, Chen T, Zhang X, Lv L, Jin C, et al. The epigenetic promotion of osteogenic differentiation of human adipose-derived stem cells by the genetic and chemical blockade of histone demethylase LSD1. Biomaterials. 2014;35(23):6015–25.
23. Ma X, Bian Y, Yuan H, Chen N, Pan Y, Zhou W, et al. Human amnion-derived mesenchymal stem cells promote osteogenic differentiation of human bone marrow mesenchymal stem cells via H19/miR-675/APC axis. Aging. 2020;12(11):10527–43.
24. Jia LF, Wei SB, Gan YH, Guo Y, Gong K, Mitchelson K, et al. Expression, regulation and roles of miR-26a and MEG3 in tongue squamous cell carcinoma. Int J Cancer. 2014;135(10):2282–93.
25. Xu R, Shen X, Si Y, Fu Y, Zhu W, Xiao T, et al. MicroRNA-31a-5p from aging BMSCs links bone formation and resorption in the aged bone marrow microenvironment. Aging Cell. 2018;17(4):e12794.
26. Zhou H, Rigoutsos I. MiR-103a-3p targets the 5' UTR of GPRC5A in pancreatic cells. RNA. 2014;20(9):1431–9.
27. Ni L, Kuang Z, Gong Z, Xue D, Zheng Q. Dihydroartemisinin Promotes the Osteogenesis of Human Mesenchymal Stem Cells via the ERK and Wnt/beta-Catenin Signaling Pathways. Biomed Res Int. 2019;2019:3456719.
28. Leng Q, Chen L, Lv Y. RNA-based scaffolds for bone regeneration: application and mechanisms of mRNA, miRNA and siRNA. Theranostics. 2020;10(7):3190–205.
29. Tang D, Tare RS, Yang LY, Williams DF, Ou KL, Oreffo RO. Biofabrication of bone tissue: approaches, challenges and translation for bone regeneration. Biomaterials. 2016;83:363–82.
30. Silini AR, Magatti M, Cargnoni A, Parolini O. Is Immune Modulation the Mechanism Underlying the Beneficial Effects of Amniotic Cells and Their Derivatives in Regenerative Medicine? Cell Transplant. 2017;26(4):531–9.
31. Wang Y, Ma J, Du Y, Miao J, Chen N. Human Amnion-Derived Mesenchymal Stem Cells Protect Human Bone Marrow Mesenchymal Stem Cells against Oxidative Stress-Mediated Dysfunction via ERK1/2 MAPK Signaling. Mol Cells. 2016;39(3):186–94.

32. Coronary Artery Disease C, Samani NJ, Deloukas P, Erdmann J, Hengstenberg C, Kuulasmaa K, et al. Large scale association analysis of novel genetic loci for coronary artery disease. Arterioscler Thromb Vasc Biol. 2009;29(5):774–80.
33. Chiu B. Multiple infections in carotid atherosclerotic plaques. Am Heart J. 1999;138(5 Pt 2):534-6.
34. Treatment of Periodontitis and Endothelial Function. N Engl J Med. 2018;378(25):2450.
35. Harismendy O, Notani D, Song X, Rahim NG, Tanasa B, Heintzman N, et al. 9p21 DNA variants associated with coronary artery disease impair interferon-gamma signalling response. Nature. 2011;470(7333):264–8.
36. Militello G, Weirick T, John D, Doring C, Dimmeler S, Uchida S. Screening and validation of lncRNAs and circRNAs as miRNA sponges. Brief Bioinform. 2017;18(5):780–8.
37. Davis HM, Pacheco-Costa R, Atkinson EG, Brun LR, Gortazar AR, Harris J, et al. Disruption of the Cx43/miR21 pathway leads to osteocyte apoptosis and increased osteoclastogenesis with aging. Aging Cell. 2017;16(3):551–63.
38. Potenza N, Russo A. Biogenesis, evolution and functional targets of microRNA-125a. Mol Genet Genomics. 2013;288(9):381–9.
39. Venugopal P, Lavu V, Rao SR, Venkatesan V. Association of microRNA-125a and microRNA-499a polymorphisms in chronic periodontitis in a sample south Indian population: A hospital-based genetic association study. Gene. 2017;631:10–5.
40. Zhou Y, Li J, Zhou K, Liao X, Zhou X, Shen K. The methylation of Notch1 promoter mediates the osteogenesis differentiation in human aortic valve interstitial cells through Wnt/beta-catenin signaling. J Cell Physiol. 2019;234(11):20366–76.
41. Wang Y, Zhang X, Shao J, Liu H, Liu X, Luo E. Adiponectin regulates BMSC osteogenic differentiation and osteogenesis through the Wnt/beta-catenin pathway. Sci Rep. 2017;7(1):3652.
42. Qu Y, Gharbi N, Yuan X, Olsen JR, Blicher P, Dalhus B, et al. Axitinib blocks Wnt/beta-catenin signaling and directs asymmetric cell division in cancer. Proc Natl Acad Sci U S A. 2016;113(33):9339–44.

Figures

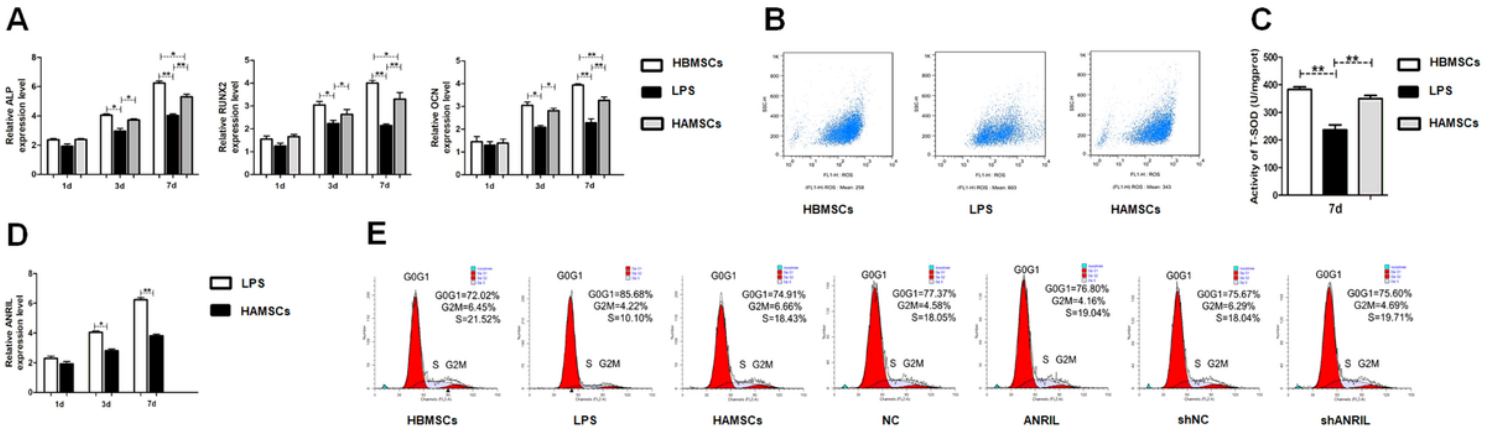

Figure 1

Osteogenic differentiation and oxidative stress level of HBMSCs cocultured with HAMSCs, lncRNA-ANRIL expression in HBMSCs and effects of lncRNA-ANRIL on proliferation of HBMSCs. A, Relative mRNA expressions in HBMSCs were measured by RT-PCR analysis. B and C, ROS and SOD level in HBMSCs were measured by Flow cytometry and xanthine oxidase assay kit. D, LncRNA-ANRIL expression in HBMSCs was measured by RT-PCR analysis. E, HBMSCs proliferation was demonstrated by flow cytometry. Data shown as mean ± SD. *P < 0.05 and **P < 0.01. LPS: LPS+HBMSCs; HAMSCs: HAMSCs+LPS+HBMSCs; NC: HAMSCs+LPS+HBMSCsNC ;ANRIL: HAMSCs+LPS+HBMSCsANRIL ;shNC: HAMSCs+LPS+HBMSCsshNC ;shANRIL: HAMSCs+LPS+HBMSCsshANRIL.

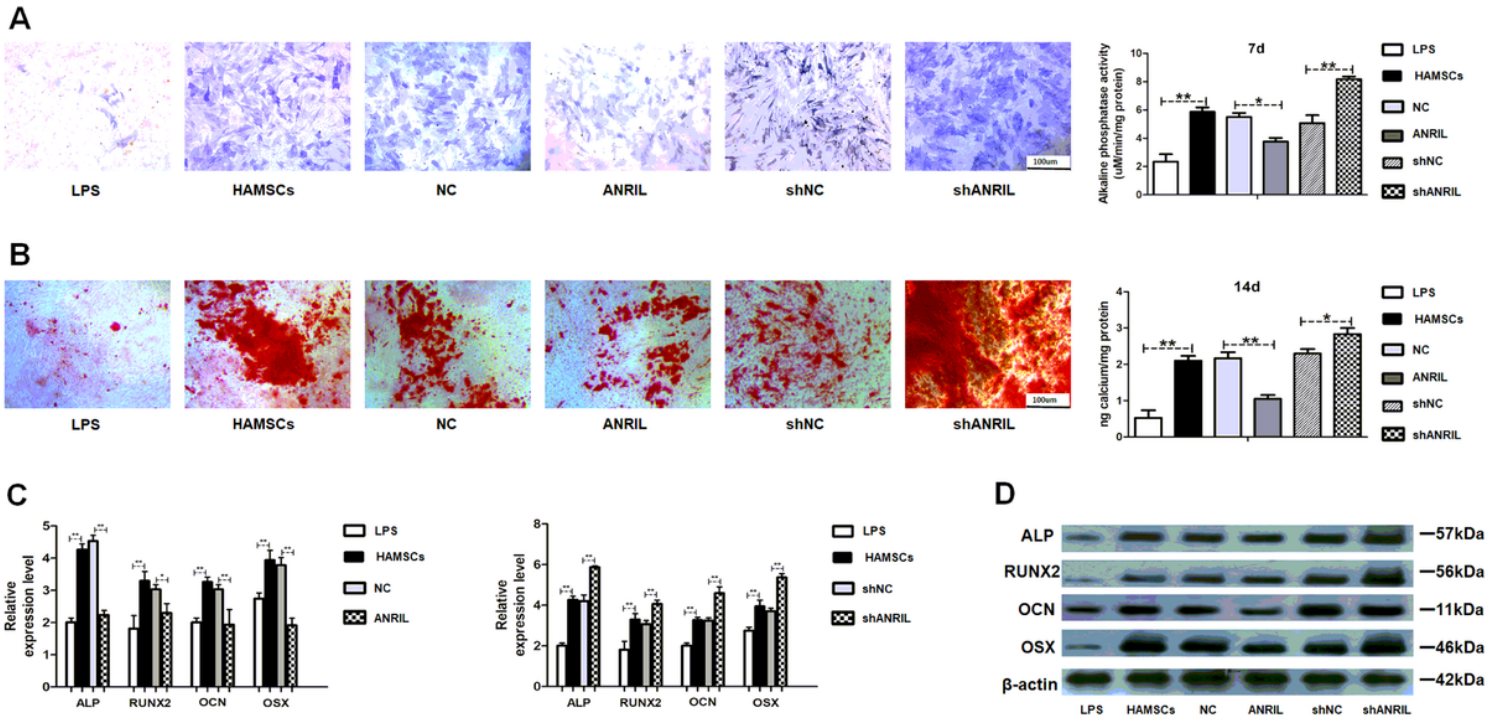

Figure 2

HAMSCs promotes osteogenesis of LPS-induced HBMSCs via downregulation LncRNA-ANRIL. A, ALP staining and activity in HBMSCs. Scale bar, 100 μm. B, Alizarin red staining and quantification in HBMSCs. Scale bar, 100 μm. C, Relative mRNA expressions in HBMSCs were measured by RT-PCR analysis. D, Relative protein levels were in HBMSCs assessed by western blot assay. Data shown as mean ± SD. *P < 0.05 and **P < 0.01. LPS: LPS+HBMSCs; HAMSCs: HAMSCs+LPS+HBMSCs; NC: HAMSCs+LPS+HBMSCsNC; ANRIL: HAMSCs+LPS+HBMSCsANRIL; shNC: HAMSCs+LPS+HBMSCsshNC; shANRIL: HAMSCs+LPS+HBMSCsshANRIL.

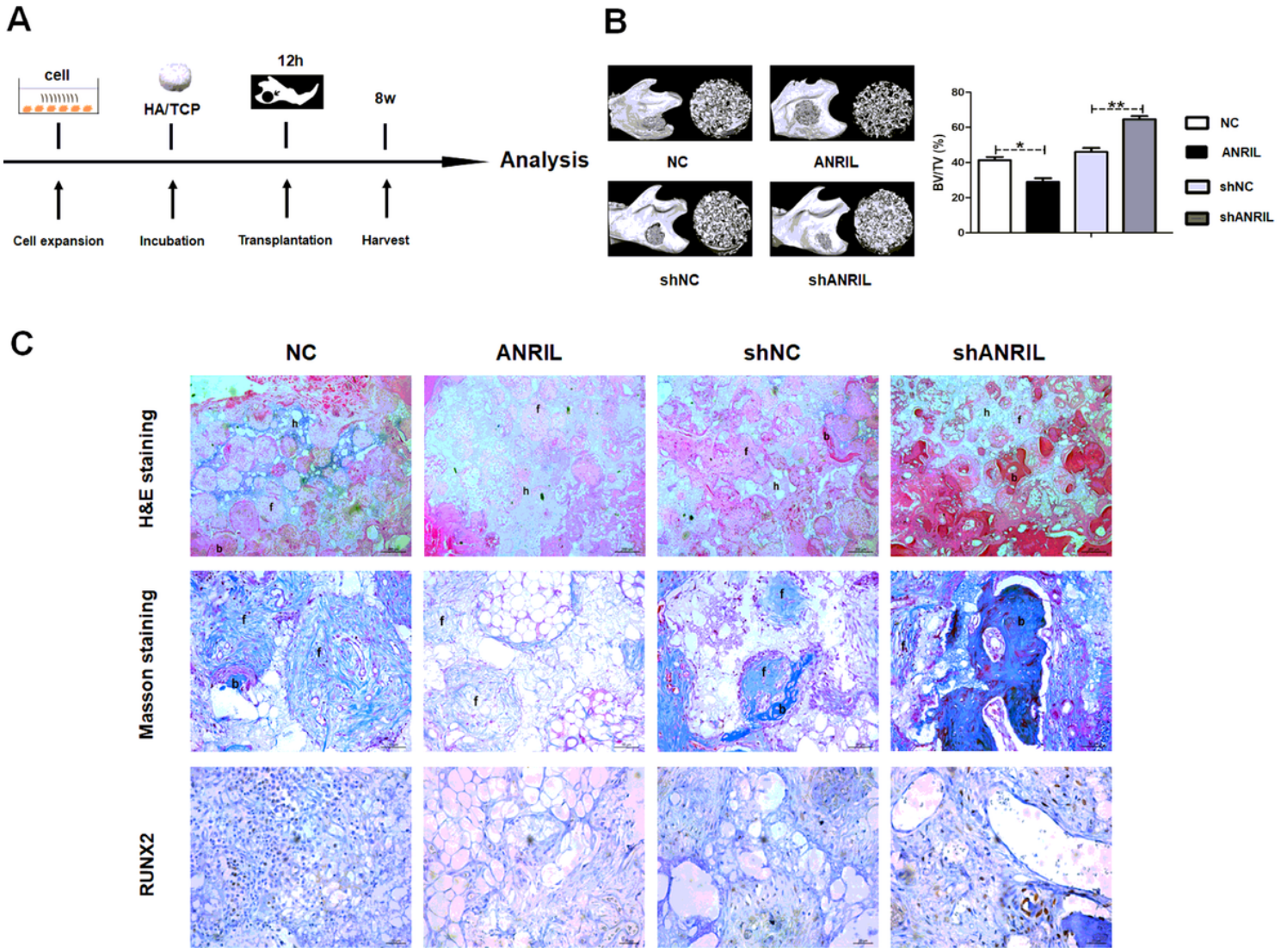

Figure 3

LncRNA-ANRIL in HBMSCs inhibits osteogenesis in vivo. A, NC, ANRIL, shNC and shANRIL groups were transplanted subcutaneously into a rat critical-sized mandibular defect model. B, Reconstructed 3D micro-CT images of the tissue-engineered bone and percentages of BV/TV. C, H&E staining, Masson staining and immunohistochemical staining of RUNX2 in each group. b: bone-like tissues, h: HA/TCP scaffold, f: fibrous. Scale bar, 200 μm. Data shown as mean ± SD. **P < 0.01. NC: HAMSCs+LPS+HBMSCsNC; ANRIL: HAMSCs+LPS+HBMSCsANRIL; shNC: HAMSCs+LPS+HBMSCsshNC; shANRIL: HAMSCs+LPS+HBMSCsshANRIL

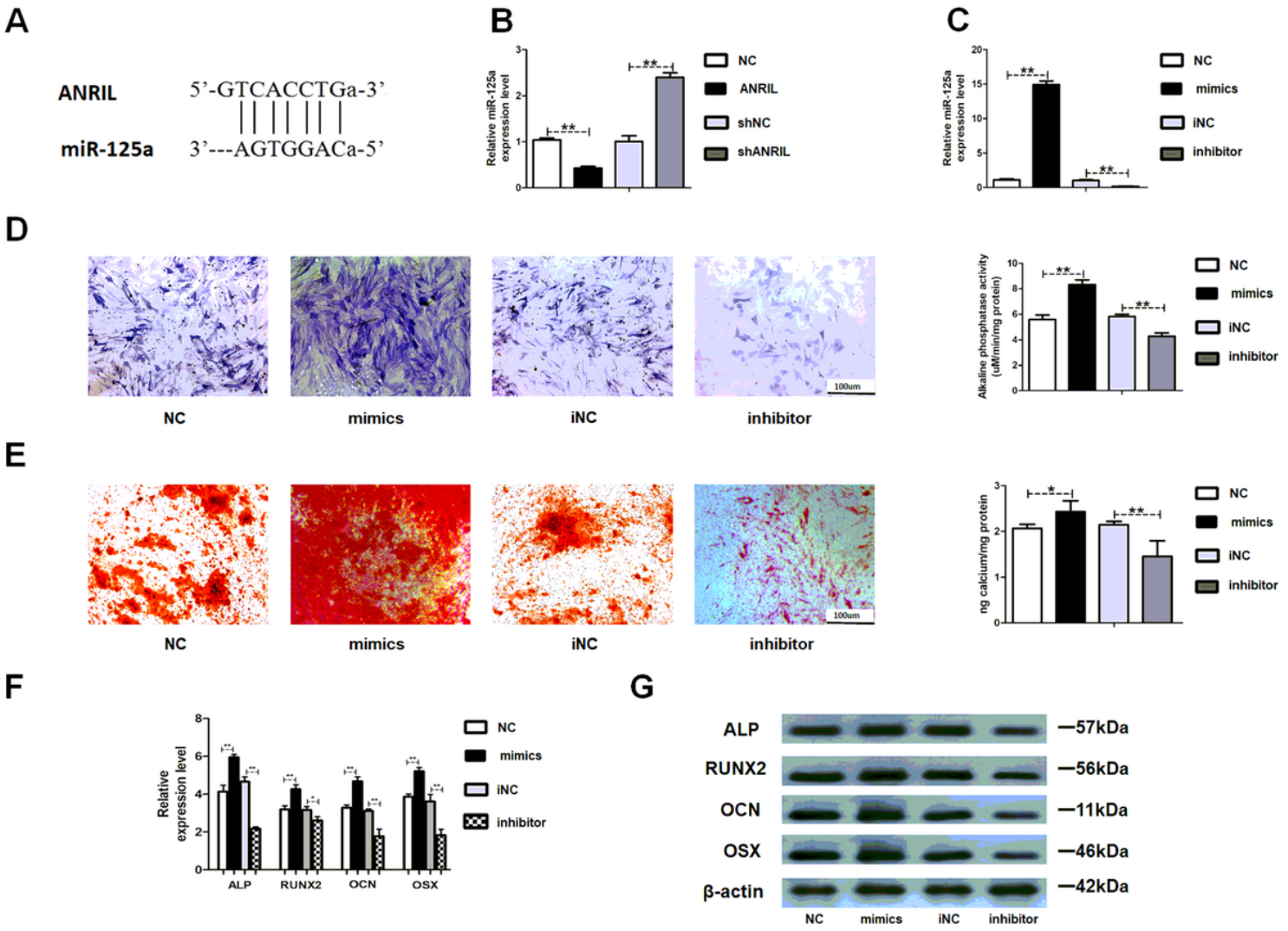

Figure 4

MiR-125a in HBMSCs is a downstream regulated by lncRNA-ANRIL and promotes osteogenic differentiation of HBMSCs. A, The binding sequence between miR-125a and ANRIL predicted by biological software. B, MiR-125a expression was measured by RT-PCR in NC, ANRIL, shNC and shANRIL groups. NC: HAMSCs+LPS+HBMSCsNC; ANRIL: HAMSCs+LPS+HBMSCsANRIL; shNC: HAMSCs+LPS+HBMSCsshNC; shANRIL: HAMSCs+LPS+HBMSCsshANRIL .C, Transfection efficacy of miR-125a was detected by RT-PCR. D, ALP staining and activity in NC, mimics, iNC and inhibitor groups. Scale bar, 100 μm. E, Alizarin red staining and quantification in NC, mimics, iNC and inhibitor groups. Scale bar, 100 μm. F, Relative mRNA expressions were measured by RT-PCR analysis. G, Relative protein levels were assessed by western blot assay. Data shown as mean ± SD. *P < 0.05 and **P < 0.01. NC: HAMSCs+LPS+HBMSCsmiR-125a NC; mimics: HAMSCs+LPS+HBMSCsmiR-125a mimics; iNC: HAMSCs+LPS+HBMSCsmiR-125a iNC; inhibitor: HAMSCs+LPS+HBMSCsmiR-125a inhibitor.

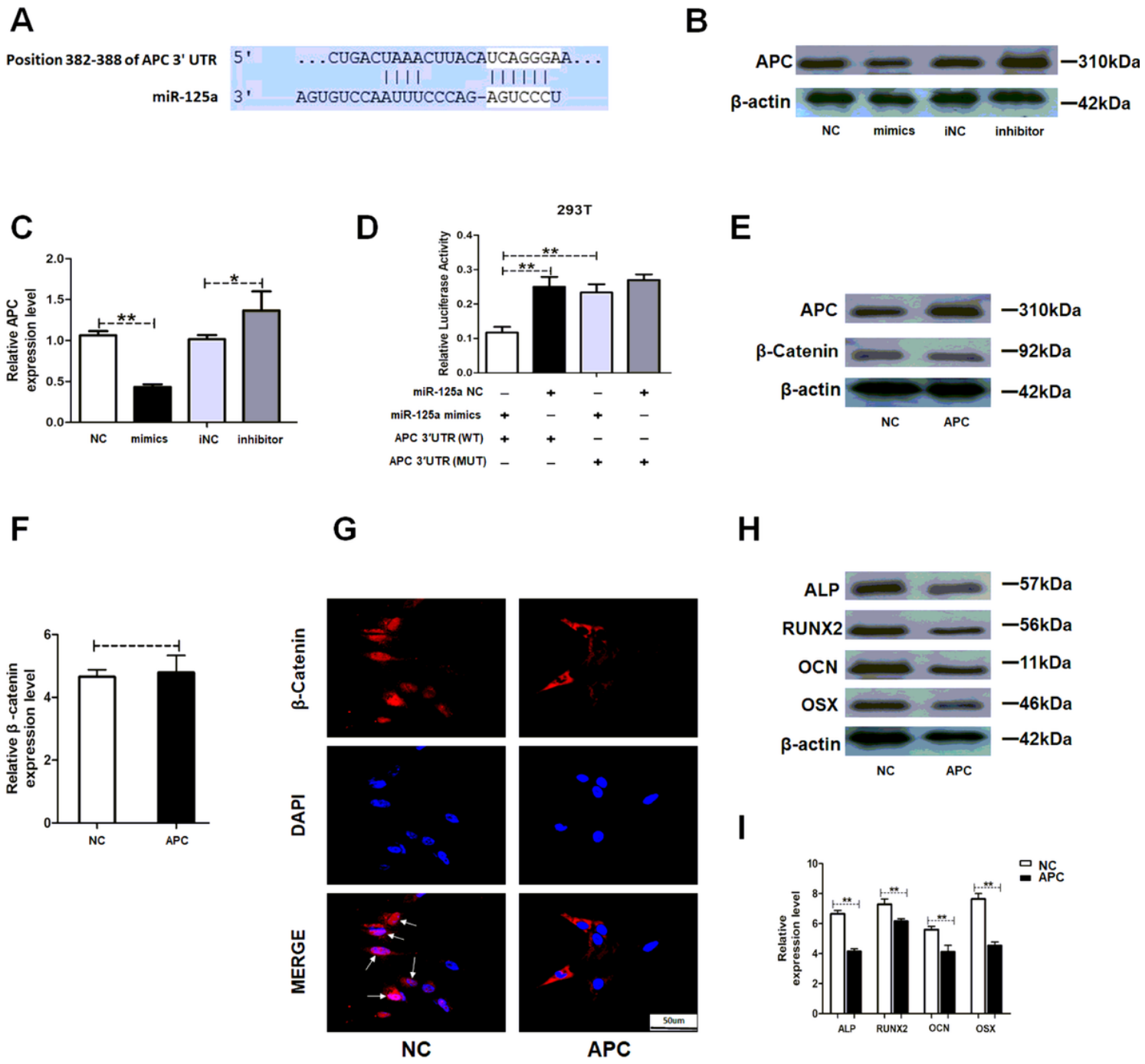

Figure 5

MiR-125a targets APC, activates Wnt/β-catenin pathway and alleviates osteogenesis. A, The potential binding sites between APC and miR-125a predicted by biological software. B, APC protein level was assessed by western blot assay in NC, mimics, iNC and inhibitor groups. C, APC mRNA expression was measured by RT-PCR analysis in NC, mimics, iNC and inhibitor groups. NC: HAMSCs+LPS+HBMSCsmiR-125a NC;mimics: HAMSCs+LPS+HBMSCsmiR-125a mimics;iNC: HAMSCs+LPS+HBMSCsmiR-125a iNC; inhibitor: HAMSCs+LPS+HBMSCsmiR-125a inhibitor. D, Luciferase reporter assay was used to validate the target in 293T cells. Relative Renilla luciferase activity was normalized to that of firefly luciferase. E, APC protein level was assessed by western blot assay in NC and APC groups. F, Relative mRNA

expression of β-catenin was measured by RT-PCR analysis in NC and APC groups. G, Immunofluorescence staining showed β-catenin location in NC and APC groups. Scale bar, 50 μm. H, Relative protein levels were assessed by western blot assay in NC and APC groups. I, Relative mRNA expressions were measured by RT-PCR analysis in NC and APC groups. NC: HAMSCs+LPS+HBMSCsAPC NC; APC: HAMSCs+LPS+HBMSCsAPC . Data shown as mean ± SD. *P < 0.05 and **P < 0.01.

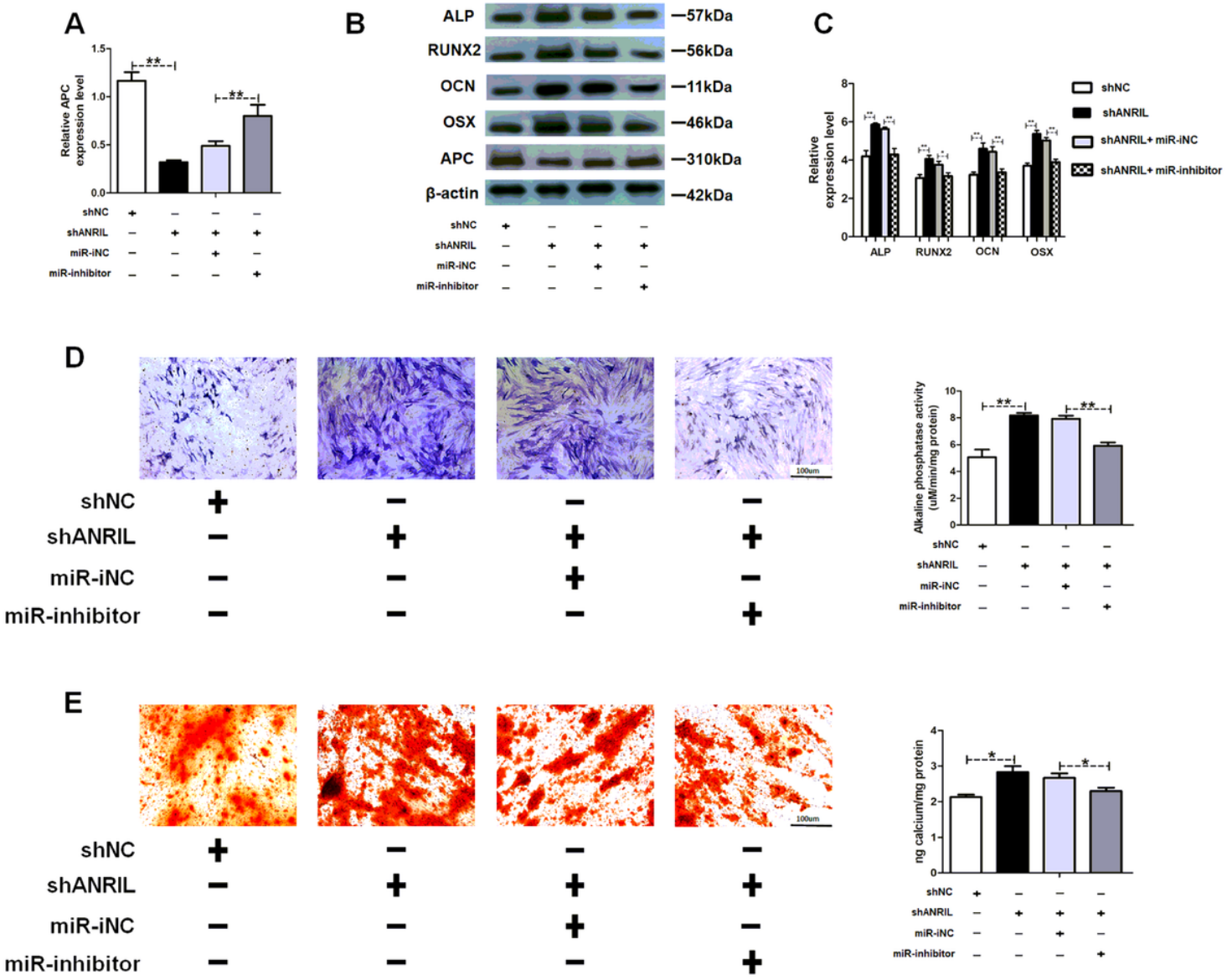

Figure 6

MiR-125a inhibitor could suppress the shANRIL mediated positive effects. A, APC mRNA expression was measured by RT-PCR analysis. B, Protein levels were assessed by western blot assay. C, Relative mRNA expressions were measured by RT-PCR analysis. D, ALP staining and activity in each group. Scale bar, 100 μm. E, Alizarin red staining and quantification in each group. Scale bar, 100 μm. Data shown as mean ± SD. *P < 0.05 and **P < 0.01.

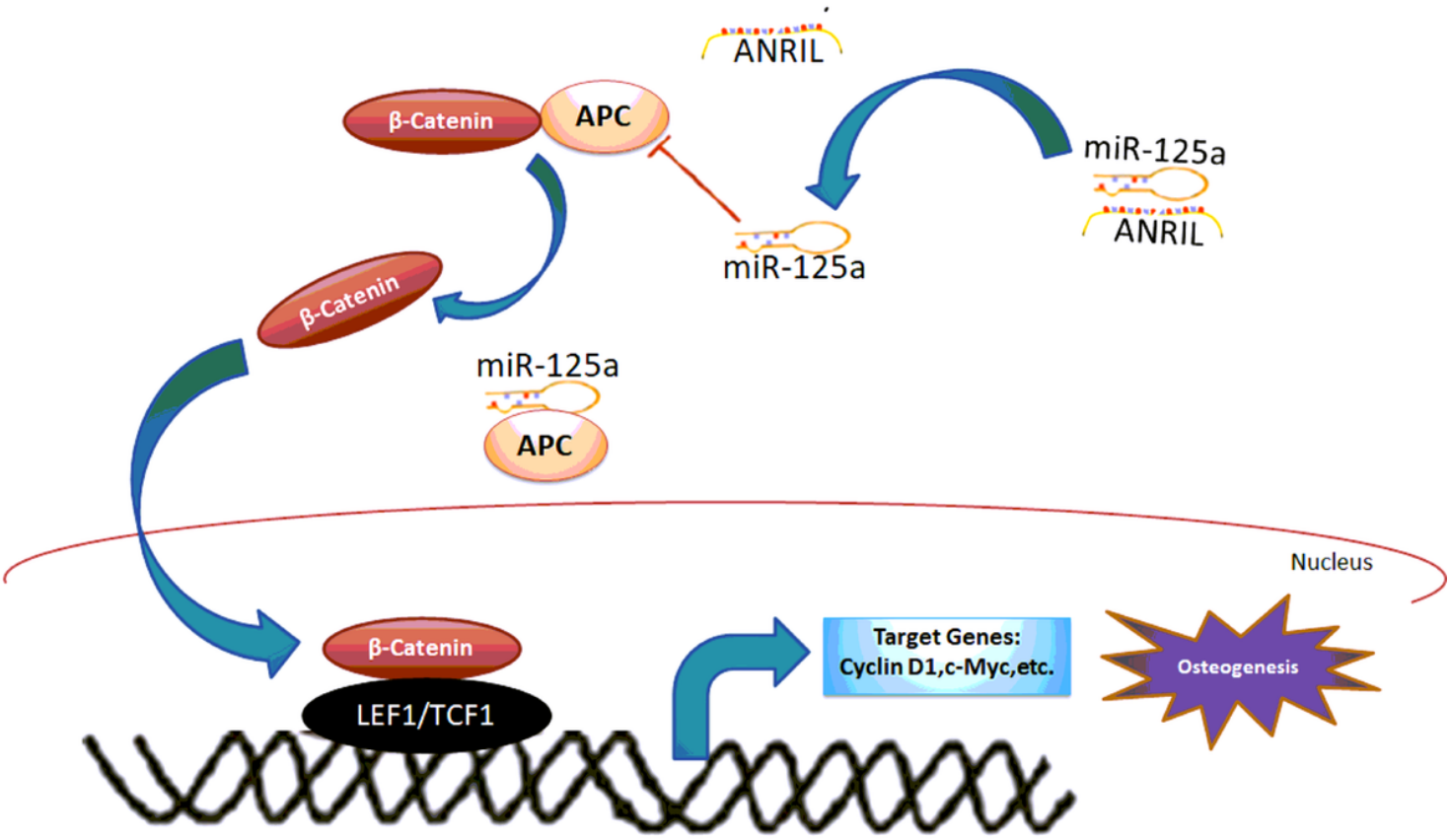

Figure 7

The schematic working model for lncRNA-ANRIL /miR-125a/APC/β-catenin axis in the regulation of LPS-induced HBMSCs osteogenesis.